Electronic Supplementary Information (ESI)

Selective recognition of Hg^{2+} ions in aqueous solution by a Cd^{II}-based metal-organic framework with good stability and vacant coordination sites

Xiao-Qin Cao,[a] Wei-Peng Wu,[a] Qiang Li,[a] Teng-Fei Zheng,[a] Yong-Qiang Chen,[b]* Jing-Lin Chen,[a] Sui-Jun Liu,[a]* and He-Rui Wen[a]

[a]School of Chemistry and Chemical Engineering, Jiangxi Provincial Key Laboratory of Functional Molecular Materials Chemistry, Jiangxi University of Science and Technology, Ganzhou 341000, Jiangxi Province, P.R. China

[b]Department of Chemistry and Chemical Engineering, Jinzhong University, Jinzhong 030619, Shanxi Province, P.R. China

*Corresponding authors. E-mail: sjliu@jxust.edu.cn (S.-J. Liu), chenyongqiang@jzxy.edu.cn (Y.-Q. Chen)

Table S1. Crystal data and structure refinements for **JXUST-28**.

Complex	**JXUST-28**
formula	$C_{18}H_{12}N_6O_6S_2Cd$
M_r	584.82
T (K)	293(2)
crystal system	Triclinic
space group	$P\bar{1}$
a (Å)	10.1318(3)
b (Å)	10.4983(3)
c (Å)	10.9116(3)
α (°)	105.487(1)
β (°)	97.662(1)
γ (°)	99.918(1)
V (Å^3)	1082.09(5)
Z	2
F(000)	572.0
D_{calc} (g cm^{-3})	1.783
μ (mm^{-1})	1.251
Reflections collected/unique	13525/3779
R_{int}	0.0177
R_1[a]/wR_2[b] [I>2σ(I)]	0.0357/0.1074
R_1[a]/wR_2[b] (all data)	0.0382/0.1099
GOF on F^2	1.086

[a]$R_1 = \Sigma(||F_0| - |F_C||)/\Sigma|F_0|$. [b]w$R_2 = [\Sigma w(|F_0|^2 - |F_C|^2)^2/(\Sigma w|F_0|^2)^2]^{1/2}$.

Table S2. Selected bond lengths (Å) and angles (°) for **JXUST-28**[a]

Cd1—O1	2.239(3)	Cd1—O2	2.648(4)
Cd1—N1^{i}	2.299(4)	Cd1—O4^{ii}	2.345(3)
Cd1—N4	2.301(4)	O3—Cd1^{v}	2.499(3)
Cd1—O3^{iii}	2.418(3)	O3—Cd1^{iii}	2.418(3)
Cd1—O3^{ii}	2.499(3)	N1—Cd1^{iv}	2.299(4)
O1—Cd1—N1^{i}	89.38(15)	N1^{i}—Cd1—O2	95.10(15)
O1—Cd1—O2	52.29(12)	N1^{i}—Cd1—O4^{ii}	94.83(13)
O1—Cd1—O4^{ii}	140.82(12)	N1^{i}—Cd1—N4	176.36(14)
O1—Cd1—N4	93.61(15)	N1^{i}—Cd1—O3^{iii}	89.20(13)
O1—Cd1—O3^{ii}	165.16(12)	N1^{i}—Cd1—O3^{ii}	86.44(13)
O1—Cd1—O3^{iii}	87.64(12)	N4—Cd1—O2	88.37(15)
O4^{ii}—Cd1—O2	88.53(11)	N4—Cd1—O4^{ii}	84.16(13)
O4^{ii}—Cd1—O3^{ii}	53.86(11)	N4—Cd1—O3^{iii}	88.85(13)
O4^{ii}—Cd1—O3^{iii}	131.27(11)	N4—Cd1—O3^{ii}	90.16(13)
O3^{iii}—Cd1—O2	139.52(11)	O3^{iii}—Cd1—O3^{ii}	78.08(12)
O3^{ii}—Cd1—O2	142.29(11)		

[a]Symmetry codes: (i) *x*-1, *y*, *z*-1; (ii) *x*, *y*-1, *z*; (iii) -*x*, -*y*+2, -*z*; (iv) *x*+1, *y*, *z*+1; (v) *x*, *y*+1, *z*.

Table S3. SHAPE analysis of Cd^{II} ion in **JXUST-28**.

ion	**label**	**shape**	**sym**	**distortion(τ)**
	HP-7	Heptagon	D_{7h}	30.173
	HPY-7	Hexagonal pyramid	C_{6v}	21.608
	PBPY-7	Pentagonal bipyramid	D_{5h}	**2.030**
Cd1	COC-7	Capped octahedron	C_{3v}	9.042
	CTPR-7	Capped trigonal prism	C_{2v}	6.911
	JPBPY-7	Johnson pentagonal bipyramid J13	D_{5h}	4.857
	JETPY-7	Johnson elongated triangular pyramid J7	C_{3v}	20.558

Table S4. The summary of the stability of some representative materials for the recognition and removal of Hg^{2+}.

Materials	Metal Ion	Testing condition	Stability	Ref.
NH_2-MIL-53(Al)	Al(III)	pH = 1-14 (8 h)	acid-base stability	S1
AH-COF		pH = 3–13 solvents ($CHCl_3$, THF, DMF, DMSO, acetone, H_2O)	acid-base stability thermal stability (300 °C) solvent stability	S2
$\{[Zn(L)(A)]\cdot DMF\}_n$	Zn(II)	pH = 3-11 organic solvents (EtOH, acetone, MeOH, MeCN, THF, DMF, DMA, 1,4-dioxane) (12h)	water stability thermal stability (300 °C) organic solvent stability acid base stability	S3
Zn-TPTC	Zn(II)		thermal stability (350 °C)	S4
$Tb(TATAB)\cdot(DMF)_4(H_2O)(MeOH)_{0.5}$	Tb(III)		water stability	S5
UiO-66@Butyne	Zr(IV)	H_2O, acetone, benzene, DMF (24 h)	solvent stability	S6
$\{[Ni1.5(L)(4,4'\text{-azobpy})(H_2O)]\cdot 6.5H_2O\}_n$	Ni(II)	pH = 1-14 (48 h), solvents (DMF, CH_3CN, THF, CH_2Cl_2, CH_3COCH_3, H_2O, CH_3CN) (48 h)	solvent stability acid-base stability	S7
RuUiO-67	Zr(IV)		chemical stability	S8
$Tb_{0.6}Eu_{0.4}$-bop nanosheets	Ln(III)		thermal stability (460 °C) chemical stability	S9
TMU-31, TMU-32	Zn(II)	water-stability (3 days)	water-stability	S10
Zn-MOF	Zn(II)	pH = 3-7 (24 h)	acid-base stability	S11
JXUST-28	Cd(II)	boiling water (5 d) pH = 2-12 (24 h) solvents (CH_2Cl_2, DMF, DMAc, MeOH, THF, MeCN, EtOH, H_2O and acetone) (24 h)	thermal stability (370 °C) boiling water stability solvent stability acid-base stability	This work

Table S5. Comparison of different MOF materials for detecting Hg^{2+}

Sensors	**Limit of detection (LOD)**	**Ref.**
NH_2-MIL-53(Al)	1.5×10^{-9} M	S1
RuUiO-67	5.0×10^{-5} M	S8
Sm-MOF	8.7×10^{-9} M	S12
Al-MIL-53-NH_2	7.56×10^{-6} M	S13
$[Zn_2(bbmb)_2(tdc)_2]\cdot2H_2O$	1.9×10^{-7} M	S14
$\{[Zn_2(1,4\text{-bpyvna})(1,3,5\text{-BTC})(OH)]\cdot H_2O\}_n$	2.9×10^{-7} M	S15
TMU-34(-2H)	1.8×10^{-6} M	S16
$\{[Cd(BIPA)(IPA)]\cdot DMF\}_n$	5.0×10^{-7} M	S17
$\{[Co_2(L)(hfpd)(H_2O)]\cdot1.75H_2O\}_n$	4.0×10^{-6} M	S18
Eu^{3+}/CDs@MOF-253	6.5×10^{-8} M	S19
PCN-221	1.0×10^{-8} M	S20
JXUST-28	9.7×10^{-8} M	This work

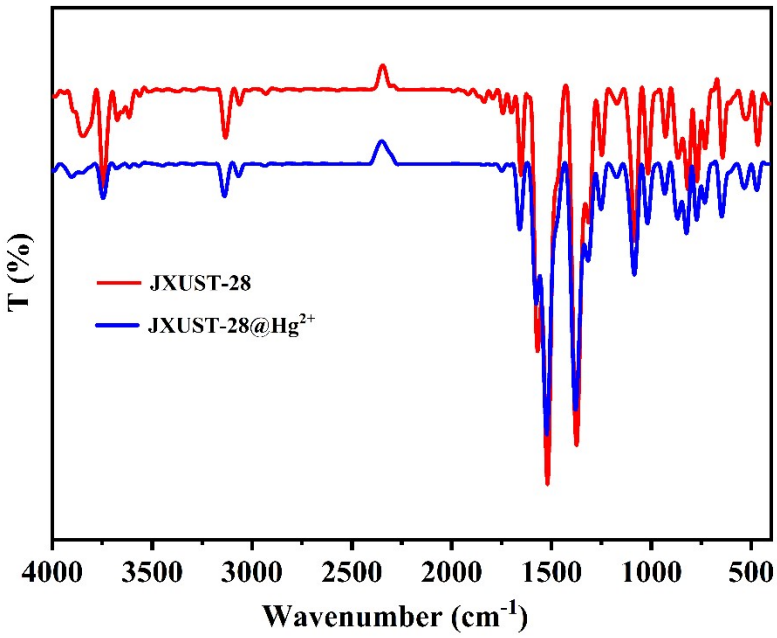

Fig. S1 IR spectra of **JXUST-28** and **JXUST-28**@Hg^{2+} at room temperature.

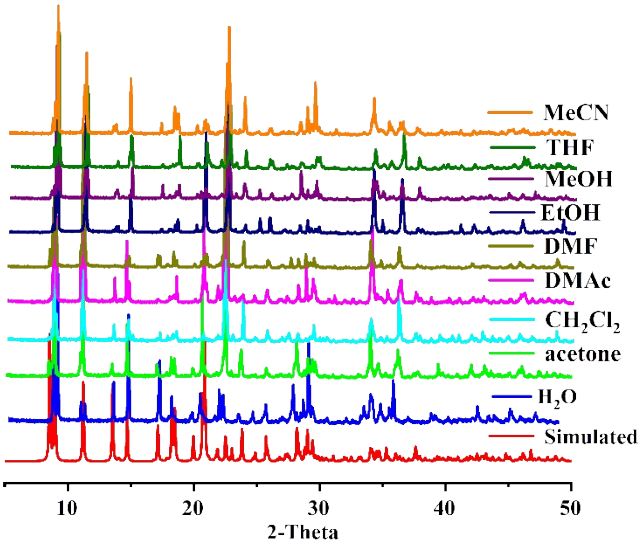

(a)

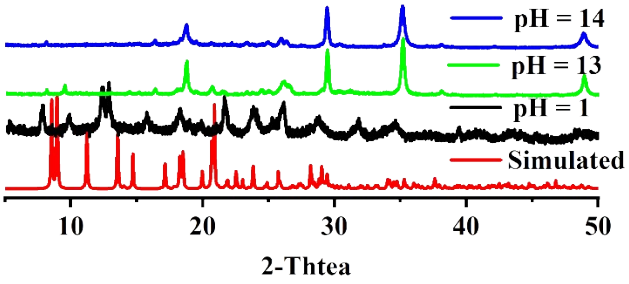

(b)

Fig. S2 (a) The simulated and experimental PXRD patterns of **JXUST-28** soaked in common organic solvents for 24 hours; (b) the simulated and experimental PXRD patterns of **JXUST-28** soaked in the aqueous solution with pH values of 1, 13 and 14 for 24 hours.

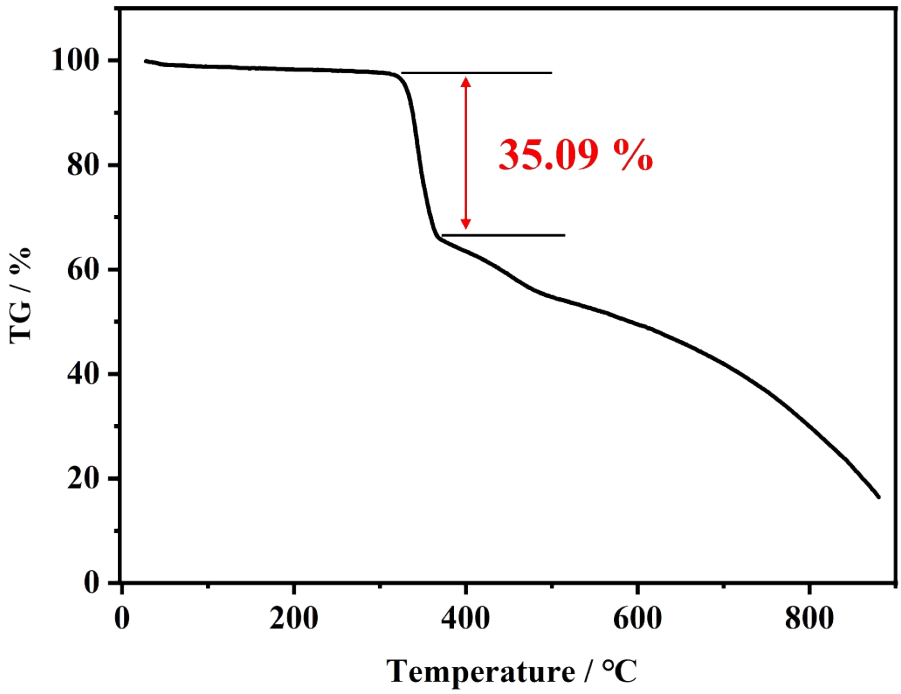

Fig. S3 The TGA curve of **JXUST-28** under N_2 atmosphere.

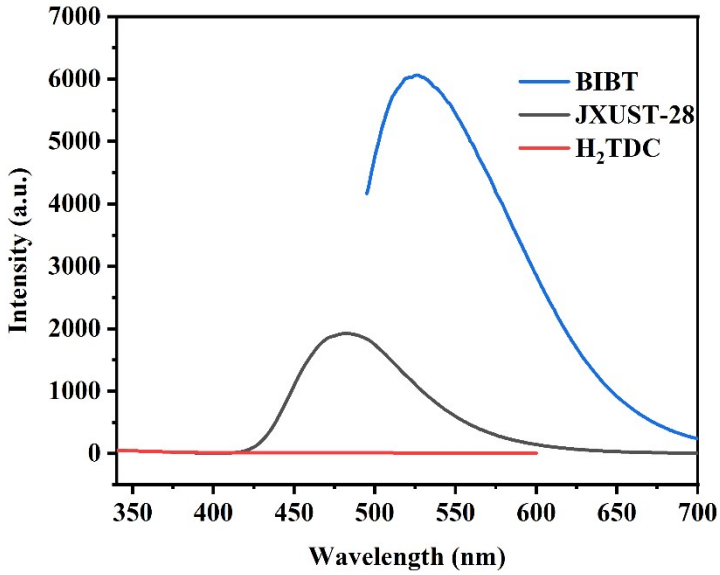

(a)

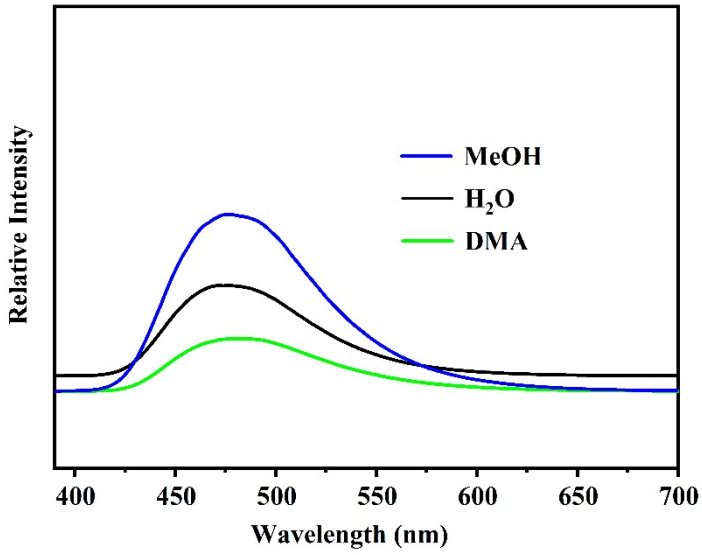

(b)

Fig. S4 (a) Solid-state emission spectra of BIBT and **JXUST-28**; (b) the emission spectra of **JXUST-28** in aqueous, DMA and MeOH solutions at room temperature.

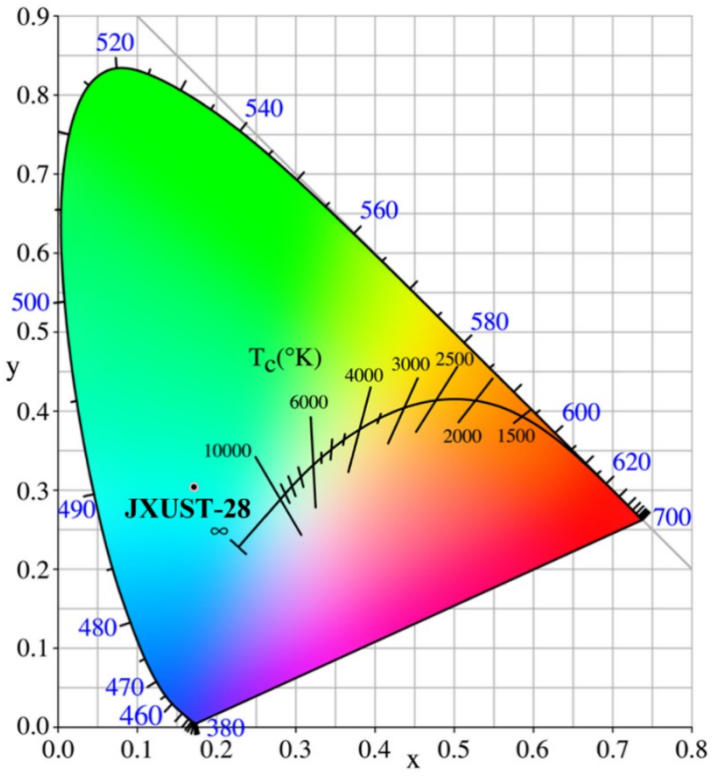

Fig. S5 CIE chromaticity diagram displaying the color coordinate of **JXUST-28**.

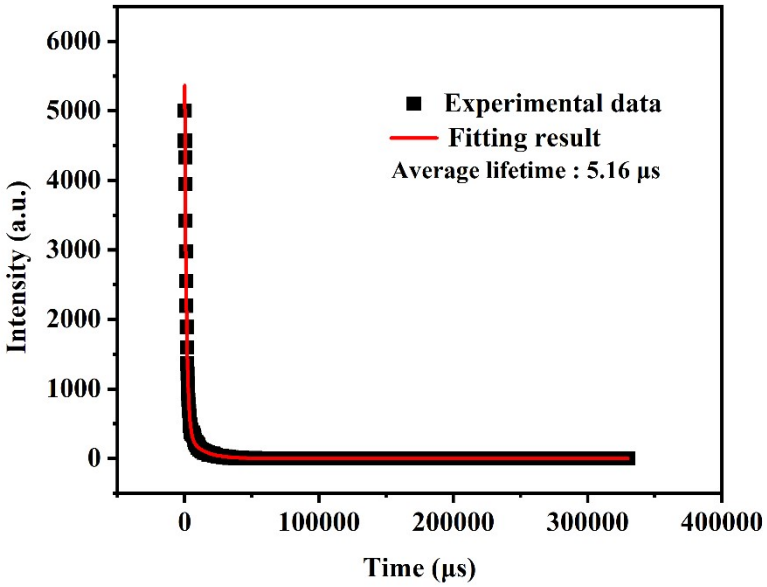

Fig. S6 The luminescence decay curve of **JXUST-28.**

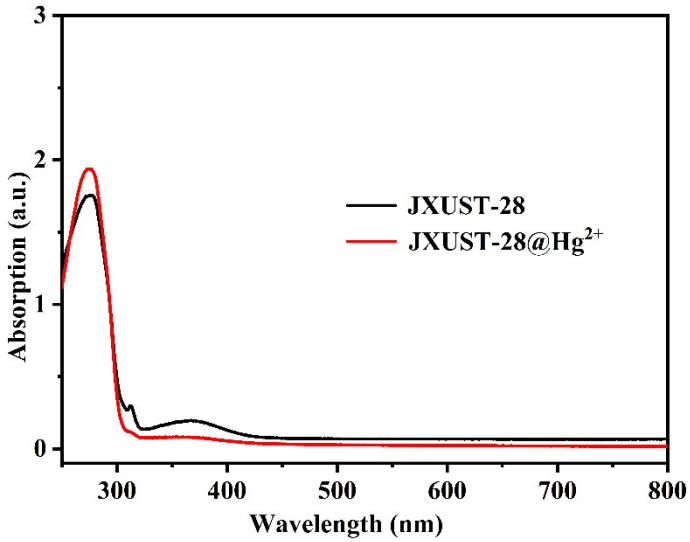

(a)

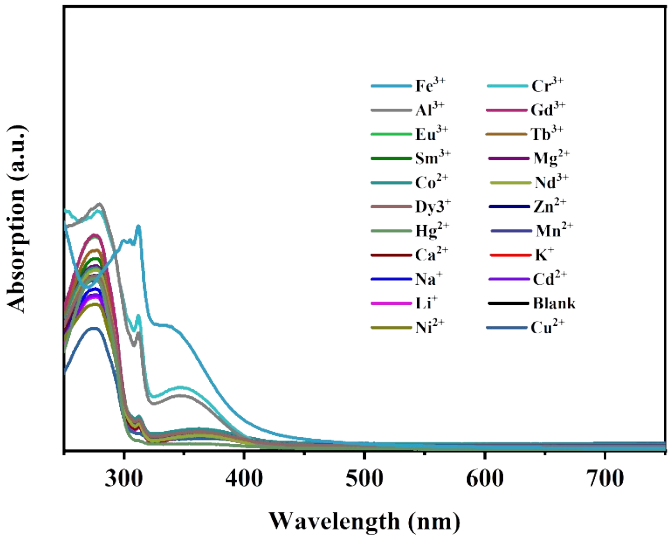

(b)

Fig. S7 (a) UV-vis absorption spectra of **JXUST-28** and **JXUST-28**@Hg^{2+}; (b) UV−vis absorption spectra of **JXUST-28** upon the addition of other metal ions.

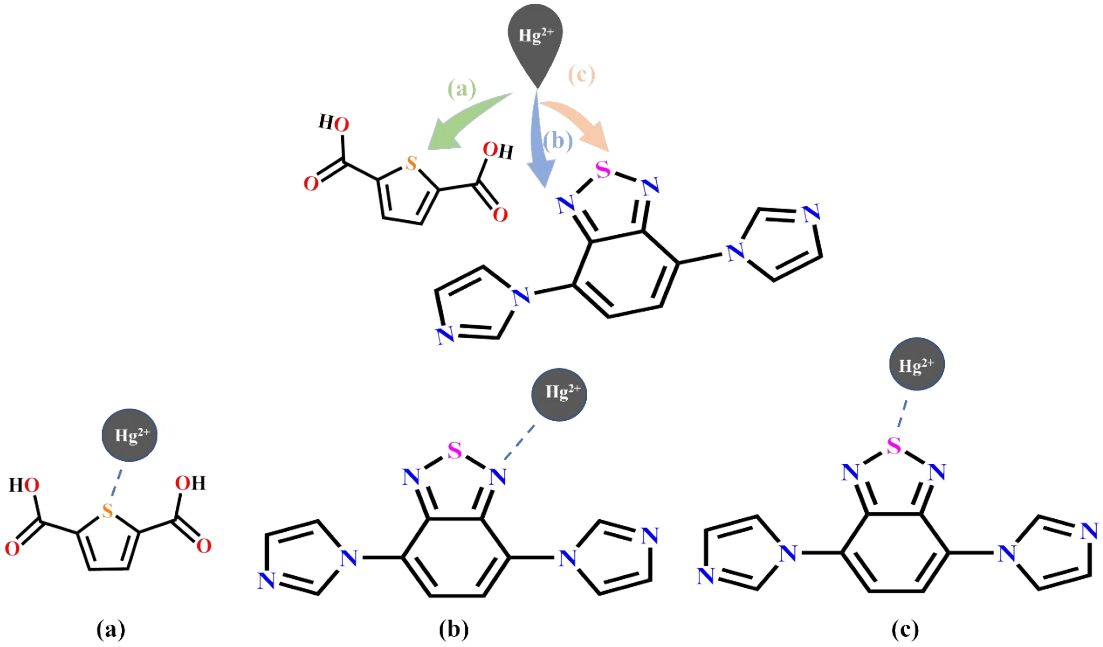

Fig. S8 The possible weak interactions between **JXUST-28** and Hg^{2+}.

References

S1. L. Zhang, J. Wang, T. Du, W. Zhang, W. Zhu, C. Yang, T. Yue, J. Sun, T. Li and J. Wang, *Inorg. Chem.*, 2019, **58**, 12573-12581.

S2. Y. X. Yu, G. L. Li, J. H. Liu and D. Q. Yuan, *Chem. Eng. J.*, 2020, **401**, 126139.

S3. X. J. Xue, Z. C. Shao, Y. Cui, T. Y. Wen, J. S. Chen, K. S. Geng, L. W. Mi and H. W. Hou, *Cryst. Growth Des.*, 2022, **22**, 1412-1420.

S4. Y. T. Wan, D. N. Zou, Y. J. Cui, Y. Yang and G. D. Qian, *J. Solid State Chem.*, 2018, **266**, 70-73.

S5. T. Xia, T. Song, G. Zhang, Y. Cui, Y. Yang, Z. Wang and G. Qian, *Chem.-Eur. J.,* 2016, **22**, 18429-18434.

S6. P. Samanta, A. V. Desai, S. Sharma, P. Chandra and S. K. Ghosh, *Inorg. Chem.*, 2018, **57**, 2360-2364.

S7. Z. C. Shao, C. Huang, J. Dang, Q. Wu, Y. Y. Liu, J. Ding and H. W. Hou, *Chem. Mater.*, 2018, **30**, 7979-7987.

S8. Z. Wang, J. Yang, Y. Li, Q. Zhuang and J. Gu, *Dalton Trans.*, 2018, **47**, 5570-5574.

S9. X. Wang, Z. Jiang, C. Yang, S. Zhen, C. Huang and Y. Li, *J. Hazard. Mater.*, 2022, **423**, 126978.

S10. A. Hakimifar and A. Morsali, *Inorg. Chem.*, 2019, **58**, 180-187.

S11. Z. Huang, M. Zhao, C. Wang, S. Wang, L. Dai and L. Zhang, *ACS Appl. Mater. Inter.*, 2020, **12**, 41294-41302.

S12. N. Wu, H. Guo, R. Xue, M. Wang, Y. Cao, X. Wang, M. Xu and W. Yang, *Colloid. Surface. A.*, 2021, **618**, 126484

S13. W. Abd El-Fattah, E. S. Al-Farraj, N. B. Hamadi, A. Alharbi and A. Shahat, *ACS Omega*, 2022, **7**, 17483-17491.

S14. W.-C. Kang, C. Han, D. Liu and G.-H. Cui, *Inorg. Chem. Commun.*, 2019, **106**, 81-85.

S15. W.-X. Li, H.-X. Li, H.-Y. Li, M.-M. Chen, Y.-X. Shi and J.-P. Lang, *Cryst. Growth. Des.*, 2017, **17**, 3948-3959.

S16. S. A. A. Razavi, M. Y. Masoomi and A. Morsali, *Inorg. Chem.*, 2017, **56**, 9646-9652.

S17**.** Z. J. Wang, L. J. Han, X. J. Gao and H. G. Zheng, *Inorg. Chem.*, 2018, **57**, 5232-5239.

S18. Y.-Q. Su, Y.-H. Qu, L. Fu and G.-H. Cui, *Inorg. Chem. Commun.*, 2020, **118**, 108013.

S19. X.-Y. Xu and B. Yan, *J. Mater. Chem. C*, 2016, **4**, 1543-1549.

S20**.** E. Moradi, R. Rahimi and V. Safarifard, *J. Solid State Chem.*, 2020, **286**, 121277.